ISSN 1063-7834, Physics of the Solid State, 2012, Vol. 54, No. 11, pp. 2212–2221. © Pleiades Publishing, Ltd., 2012.
Original Russian Text © N.B. Ivanova, M.S. Platunov, Yu.V. Knyazev, N.V. Kazak, L.N. Bezmaternykh, A.D. Vasiliev, S.G. Ovchinnikov, V.I. Nizhankovskii, 2012, published in Fizika Tverdogo Tela, 2012, Vol. 54, No. 11, pp. 2077–2085.

MAGNETISM

Effect of the Diamagnetic Dilution on the Magnetic Ordering and Electrical Conductivity in the $Co_3O_2BO_3$: Ga Ludwigite

N. B. Ivanova[a, b, *], M. S. Platunov[b, c], Yu. V. Knyazev[a], N. V. Kazak[b], L. N. Bezmaternykh[b], A. D. Vasiliev[a, b], S. G. Ovchinnikov[a, b, c], and V. I. Nizhankovskii[d]

[a] *Siberian Federal University, pr. Svobodnyi 79, Krasnoyarsk, 660041 Russia*

* *e-mail: nat@iph.krasn.ru*

[b] *Kirensky Institute of Physics, Siberian Branch of the Russian Academy of Sciences, Akademgorodok 50–38, Krasnoyarsk, 660036 Russia*

[c] *Reshetnev Siberian State Aerospace University, pr. imeni Gazety "Krasnoyarskii Rabochii" 31, Krasnoyarsk, 660014 Russia*

[d] *International Laboratory of High Magnetic Fields and Low Temperatures, Gajowicka str., 95 Wroclaw, 53-421 Poland*

Received March 6, 2012

Abstract—Single crystals of cobalt ludwigite $Co_3O_2BO_3$ with diamagnetic substitution of Ga^{3+} ions for a part of the cobalt ions have been grown by the flux method. A detailed investigation of the crystal structure and magnetic properties of the compound has been carried out. A preferred character of the occupation of nonequivalent crystallographic positions by gallium has been revealed. It has been found that the effective magnetic moment and the magnetic ordering temperature are decreased compared to those in the original crystal of the $Co_3O_2BO_3$ ludwigite. It has been noted that the pronounced magnetic anisotropy observed in the crystallographic *ab* plane of the original material of the $Co_3O_2BO_3$ composition disappears in the presence of gallium.

DOI: 10.1134/S1063783412110133

1. INTRODUCTION

In the last few years, a significantly increasing interest has been expressed by researchers in transition metal oxyborate compounds with a ludwigite structure [1–5]. The class of oxyborate compounds, on the whole, is attractive for scientific research in view of the wide variety of crystal structures formed during the synthesis. As a rule, these structures are quasi-low-dimensional and include elements in the form of zig-zag walls in ludwigites [6] or ribbons in pyroborates [7, 8] and warwickites [9]. The nonequivalence of crystallographic positions of metal ions and the hierarchical character of exchange interactions substantially complicate and enrich the picture of the magnetic behavior of the compounds under consideration. Nonequivalent lattice sites in oxyborates can be occupied by metal ions of different valences. This leads to the formation of an extremely rich picture of the internal structure of oxyborates, which eventually determines their physical properties.

Ludwigites have an orthorhombic crystal structure with symmetry space group *Pbam*. The metal ions can occupy four nonequivalent positions. The crystal structure of the ludwigite is schematically shown in Fig. 1 in the projection onto the crystallographic *ab* plane. In this figure, nonequivalent crystallographic positions of the metal ion are numbered. The number of positions *3* and *4* exceeds the number of positions *1* and *2* by a factor of two. The metal ions located in positions *1* and *3*, as well as the ions located in positions *2* and *4*, form two parallel layers. These layers are shifted with respect to each other by one-half of the lattice parameter in the *c* direction, which is approximately equal to 1.5 Å. The triangular BO_3 groups lie in the same plane as the metal ions located in positions *2*

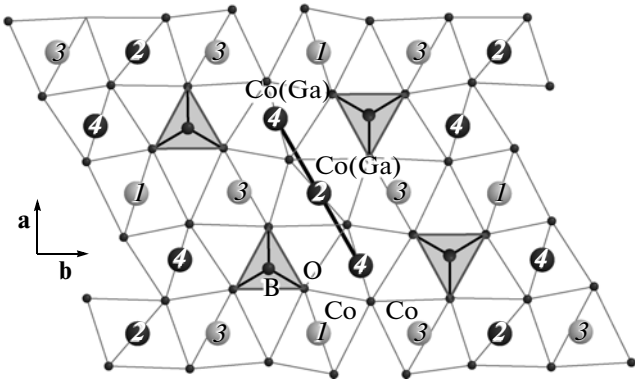

Fig. 1. Zig-zag walls in the crystal structure of the ludwigite. Large circles show metal ions, and numerals indicate nonequivalent crystallographic positions. The metal ions are surrounded by the oxygen octahedra. The positions containing gallium are marked in black. The BO_3 groups have a triangular structure with the boron ion located at the center.

and *4*. Each metal ion is located inside the distorted oxygen octahedron. The zig-zag walls formed by the edge-shared octahedra propagate along the crystallographic *c* direction.

Ludwigites contain the divalent and trivalent metal ions in the ratio of 2 : 1. The divalent and trivalent metal ions can be distributed over the crystallographic positions in different ways depending on the type of ions. In the majority of previous investigations, divalent and trivalent ions are different metal elements (for example, Cu^{2+}, Ni^{2+}, and Mg^{2+} in combination with Ga^{3+}, Al^{3+}, and Fe^{3+}) [3, 10–12]. These ludwigites are referred to as heterometallic. At present, there are only two synthesized homometallic ludwigites, namely, $Co_3O_2BO_3$ and $Fe_3O_2BO_3$ [1, 13]. The first compound in a good quality was synthesized considerably later than the second compound and, by now, has been much less studied. To date, the following has been known about the properties of the $Co_3O_2BO_3$ ludwigite.

(1) Crystals grown by the flux method have the form of fine black needles with a weight of up to 1 mg and a density of approximately 5 g/cm^3 (the lattice parameters are as follows: $a = 9.302$ Å, $b = 11.957$ Å, and $c = 2.972$ Å) [2].

(2) The material is magnetically ordered at the Néel temperature $T_N = 43$ K, and the ordering apparently has a ferrimagnetic character [6, 13, 14].

(3) The material has a pronounced uniaxial magnetic anisotropy with the easy magnetization axis along the crystallographic *b* direction [6, 14].

(4) The material is characterized by a significant magnetic rigidity [6, 14].

(5) The substitution of nonmagnetic ions, for example, Ti^{4+} [15] or Mg^{2+} and Ga^{3+} [16], for a part of cobalt ions leads to the disappearance of long-range magnetic order and the formation of a state similar to the spin glass.

(6) At low temperatures, the $Co_3O_2BO_3$ compound is a magnetic dielectric; as the temperature increases, the compound undergoes a gradual transition from hopping conduction to conduction of the activation type [2].

This work continues our previous investigations [1, 2, 6, 14, 16, 17] and has been devoted to the study of the magnetic and transport properties of the cobalt oxyborate $Co_3O_2BO_3$ with diamagnetic substitution of Ga^{3+} ions for a part of the cobalt ions.

2. SYNTHESIS TECHNOLOGY AND SAMPLES

Single crystals of the $Co_3O_2BO_3$: Ga ludwigite under investigation were grown by the flux method using the technology described earlier in [3] for the synthesis of transition metal ludwigites. The initial reactants with a total weight of 50 g were taken in the molar ratios $Bi_2Mo_3O_{12} : B_2O_3 : CoO : Na_2Co_3 : Co_2O_3 = 3 : 2 : 4 : 3 : 3$. In order to obtain the substituted composition, a part of the cobalt oxide Co_2O_3 was replaced with the gallium oxide Ga_2O_3. The solution melt was prepared in a platinum crucible by successive melting at temperatures in the range from 900 to 1000°C. In the crystallization furnace with an inhomogeneous temperature field, the crucible was mounted so that, at a temperature of 900°C, the vertical component of the temperature gradient in the solution melt was less than 1°C/cm. For the complete dissolution and homogenization, the composition was held for 3 h at a temperature of 1100°C. Then, the solution melt was subjected to a two-step cooling: a rapid cooling to 960°C at the first stage and a slow cooling at the second stage with a rate of 12°C per day for three days. During the second stage, spontaneously nucleated single crystals grew. Then, the solution melt was poured out. The single crystals grown up on the walls of the crucible were freed from the remaining solution melt by etching in a 20% aqueous solution of nitric acid. As a result, single crystals were obtained in the form of rectangular parallelepipeds strongly elongated along the crystallographic *c* axis.

The grown crystals have the form of smooth black needles up to 5 mm in length. The cross-sectional area of the crystal is no less than 0.5×0.5 mm. The crystal shape makes it easy to determine the crystallographic *c* direction. In order to determine the other crystallographic directions, it is necessary to choose crystals with an approximately plate-like shape. The short side of the cross section of the crystal coincides with the crystallographic *b* direction.

3. X-RAY DIFFRACTION

The crystal structure of the $Co_3O_2BO_3$: Ga ludwigite was investigated using a SMART APEX II single-crystal X-ray diffractometer (MoK_α radiation, CCD detector). X-ray diffraction was performed on a single-crystal sample at room temperature. The X-ray diffraction pattern of the single-crystal sample is shown in Fig. 2. The crystal structure of the sample under investigation is resolved in detail. The X-ray diffraction data are presented in Table 1. The introduction of gallium into the initial cobalt ludwigite causes a slight increase in the unit cell volume within the limits of 4%.

The atomic coordinates, site occupancy factors (SOF) for nonequivalent crystallographic positions, and isotropic displacement parameters are presented in Table 2. As can be seen from these data, the gallium ions are located only in crystallographic sites *4* and *2*. Site *4* is most preferred. It is filled with gallium by more than half. This situation is typical of substituted cobalt ludwigites. As was shown previously, this site is most easily occupied by iron [4, 6, 17], copper [18], and manganese [19] ions. The site occupation scenario observed in the present work almost completely coincides with the scenatio in the case with iron that plays the role of a substituting ion. The iron ions, the

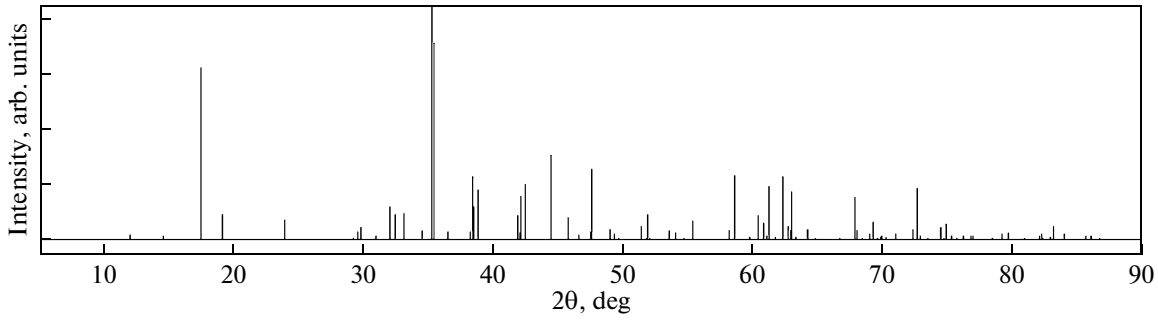

Fig. 2. X-ray diffraction pattern of the substituted cobalt ludwigite $Co_{2.4}Ga_{0.6}O_2BO_3$.

like gallium ions, also obviously "prefer" site *4* and, to a lesser extent, occupy site *2*. The crystallographic sites occupied by ions of different types are shown in Fig. 3, where the positions of the ions are indicated in the projections onto the planes *ac* and *bc*. It can be seen that sites *2* and *4* containing the gallium ions are located predominantly in the *ab* planes and separated by parallel layers containing only the cobalt ions.

With the knowledge of the site occupancy factors for nonequivalent crystallographic positions, we can refine the chemical formula of the compound under investigation. Sites *4* and *2* are filled with gallium by 54.4% and 15.5%, respectively. Hence, the chemical formula of the composition can be written as $Co_{2.38}Ga_{0.62}O_2BO_3$ or, in round numbers, as $Co_{2.4}Ga_{0.6}O_2BO_3$. In this case, the ratio of the cobalt concentration to the gallium concentration is equal to 4 : 1. In other words, the cobalt content in the sample reaches approximately 80% of the amount of the metal ions, whereas the gallium content amounts to only 20%.

Table 1. X-ray diffraction data for the $Co_3O_2BO_3$: Ga sample

Chemical formula	$Co_{2.4}Ga_{0.6}O_2BO_3$
Molar weight	337.32
Wavelength, Å	0.71073
Temperature, K	296
Crystal structure	Orthorhombic
Symmetry space group	*Pbam*
Unit cell parameters:	
a, Å	9.2962
b, Å	12.1929
c, Å	3.0275
V, Å^3	343.16
Density (calculated), g/cm^3	3.265
Size of the studied crystal, mm	3.4 × 0.14 × 0.12
F(000)	314.0
Absorption coefficient, mm^{-1}	10.956
Diffraction angle θ, deg	2.76–28.99
Correction	Gaussian
Results of the least-squares analysis	
Data/absorption/parameters	537/0/60
Goodness of fit	1.202
Final *R*-factors:	
*R*1	0.0138
*wR*2	0.0295

The selected interionic distances in the ludwigite structure are presented in Table 3. Here, we can distinguish three groups of distances. The first group of distances includes the distances between ions in the BO_3 triangle. These distances are the shortest ones; thus, the BO_3 group is characterized by the strong ionic bonding.

The second group of distances includes the distances between the metal ions. The nearest distances between any sites that contain the metal ions are of the order of three angstroms. The shortest distance is observed for sites *2* and *4*. It is slightly smaller than 3 Å. This distance is close to the radius of the direct exchange interaction between the ions. All the distances between the metal ions in the structure of the $Co_{2.4}Ga_{0.6}O_2BO_3$ compound are slightly larger than those in the structure of the original material of the $Co_3O_2BO_3$ composition.

The third group of distances includes the distances between the metal ion and oxygen (Fig. 4). The oxygen ions can occupy the five sites O1–O5, which are crystallographically nonequivalent. As can be seen from the interatomic distances presented in Table 3, each metal ion is located in an oxygen octahedron with a different degree of distortion. In particular, for example, the cobalt ion located in site *1* is characterized by four identical Co1–O4 distances. Let us assume that the square formed by the O4 ions is the base of the octahedron. At the same time, two Co1–O2 distances in the direction perpendicular to the base of the octahedron are somewhat shorted. Then, the O2–Co1–O2 direction can be considered as the principal axis of the octahedron. In this case, the oxygen octahedron itself will be compressed along the principal axis. Similarly, for the Co2 ion, the principal axis of the octahedron will coincide with the O3–Co2–O3 direction, which is characterized by somewhat shorter interatomic distances as compared to those in the

square formed by the O5 ions, where all the Co2–O5 distances are equal to each other. The situation with the Co3 and Co4 ions is more complicated, because both these ions are surrounded by four nonequivalent oxygen sites rather than by two nonequivalent oxygen sites. However, based on the data presented in Table 3, we can conclude that, for the Co3 ion, the Co3–O1 and Co3–O3 distances are almost identical to each other; therefore, the O2–Co3–O5 direction can be regarded as the principal axis of this octahedron. Hence, three octahedra surrounding the sites occupied by the Co1–Co3 ions will be compressed with respect to their principal axes. A quite different situation occurs with the oxygen octahedron surrounding site *4*, because, in this case, four identical interatomic distances could not be revealed and the octahedron could not be considered to be elongated or compressed. Therefore, the principal axis of this octahedron was chosen arbitrarily as the direction from the O1 ion to the O4 ion. For all the positions of the metal ions, the directions of the metal ion–oxygen bonds, as well as the directions corresponding to the principal axes of the oxygen octahedra, are approximately identical. They approximately coincide with the direction of the diagonal of the *ab* face of the unit cell of the crystal. In Fig. 4, the directions of the principal axes of the oxygen octahedra are indicated in bold. With the knowledge of the parameters of the octahedra, it is possible to calculate the gradient of the electric field induced by them (i.e., the electric field gradient). As was done in our recent work [17], the electric field gradient was calculated according to the formula $V_{zz} = \sum 2e\frac{3\cos^2\beta - 1}{r^3}$ with the inclusion of the first coordination sphere. Here, V_{zz} is the electric field gradient in the direction of the principal axis of the oxygen octahedron, β is the angle between this axis and the direction toward the neighboring oxygen ion, e is the elementary charge, and r is the distance between the metal ion and oxygen. The obtained results are presented in Table 4.

Table 2. Atomic coordinates, site occupancy factors (SOF) for nonequivalent crystallographic positions, and isotropic thermal parameters U for the $Co_3O_2BO_3$: Ga sample

Atom	*x/a*	*y/b*	*z/c*	SOF	U, Å^2
Co1	0	0.50000	0.50000	0.25000	0.00613
Co2	0.50000	0.50000	0	0.21125	0.00667
Ga2	0.50000	0.50000	0	0.03875	0.00667
Co3	0.49891	0.72080	0.50000	0.50000	0.00630
Co4	0.23761	0.616396	0	0.22800	0.00602
Ga4	0.26016	0.616396	0	0.27200	0.00602
O1	0.34462	0.76297	0	0.50000	0.00970
O2	0.10805	0.64306	0.50000	0.50000	0.01030
O3	0.38478	0.57811	0.50000	0.50000	0.01000
O4	0.15312	0.45852	0.50000	0.50000	0.01390
O5	0.38478	0.57811	0.50000	0.50000	0.01390
B	0.7712	0.63849	0	0.50000	0.00820

According to the data presented in this paper, the gallium ions predominantly occupy the sites characterized by the lowest value of the electric field gradient. The same pattern was noted in the case of the substitution of iron ions for cobalt ions in our recent studies [6, 17].

4. MAGNETIC MEASUREMENTS

For magnetic measurements, we used a vibrating-sample magnetometer with a step motor [20]. The measurements were performed at the International Laboratory of High Magnetic Fields and Low Temperatures (Wroclaw, Poland). The temperature depen-

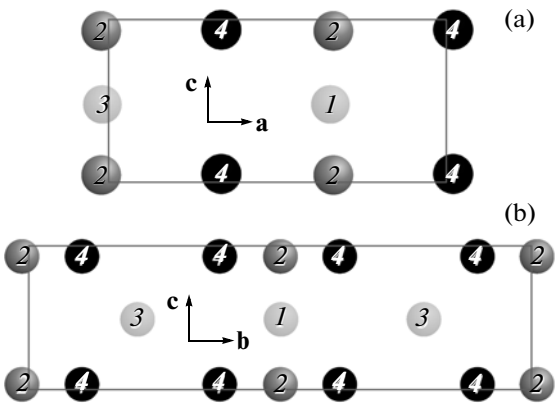

Fig. 3. Crystallographic layers containing the substituting gallium ions (sites *2* and *4*) in the $Co_{2.4}Ga_{0.6}O_2BO_3$ structure projected onto the planes (a) *ac* and (b) *bc*.

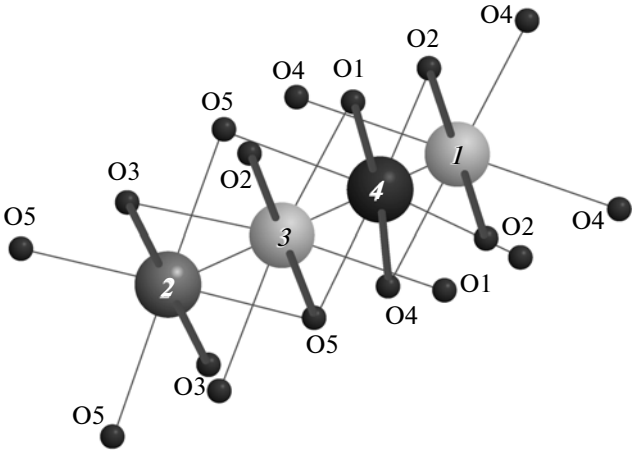

Fig. 4. Distorted oxygen octahedra surrounding the metal ions in nonequivalent sites *1–4*. The positions of the oxygen ions are also nonequivalent. The direction of the principal axes of the octahedra is shown.

Table 3. Interionic distances in the structure of the $Co_{2.4}Ga_{0.6}O_2BO_3$ compound (in Å)

Distances in the BO_3 group			
B–O1	1.382	B–O4	1.376
B–O3	1.376		
The shortest distances between the metal ions			
Co1–Co3	3.4043	Co1–Co(Ga)4	3.0306
Co(Ga)2–Co3	3.0886	Co(Ga)2–Co(Ga)4	2.8221
Co3–Co(Ga)4	3.1325		
Bond lengths in the oxygen octahedra			
Co1–O2	2.0129	Co3–O3	2.1474
Co1–O4	2.1390	Co3–O5	2.0378
Co(Ga)2–O3	2.0497	Co(Ga)4–O1	2.0454
Co(Ga)2–O5	2.0846	Co(Ga)4–O2	1.9616
Co3–O1	2.1479	Co(Ga)4–O4	2.0790
Co3–O2	1.9455	Co(Ga)4–O5	2.0931

Table 4. Principal component of the electric field gradient tensor and occupancies of gallium ion sites in the structure of the $CO_{2.4}Ga_{0.6}O_2BO_3$ compound

Parameter	Site			
	1	2	3	4
G, e/Å^3	0.2002	0.06818	0.24896	–0.0426
Ga site occupancy, %	0	15.5	0	54.4

dences of the static magnetization were measured during cooling in a zero magnetic field (the ZFC mode) at temperatures in the range from 1.8 to 300 K. The magnetic field was applied in the crystallographic *a* direction. The measurements were carried out in a magnetic field of 5 T and in the case where the residual field of the magnet was equal to 0.025 T. The magnetization curves were obtained in magnetic fields of up to 14 T in the crystallographic directions *a*, *b*, and *c*, which were determined in accordance with the X-ray diffraction data. Prior to the measurement, the single crystal was accurately weighed using a DV 215CD semi-micro balance. The single crystal was mounted on a plexiglas holder. The temperature dependence of the magnetization of the holder was measured separately and then was subtracted from the integrated signal. The correction for the magnetization of the holder accounted for 10% of the magnetization of the sample. When the measurements were performed in the crystallographic *b* direction, we evaluated the effect of the demagnetization associated with the shape of the sample. Taking into account all the errors introduced during the weighing of the single crystal, the subtraction of the signal from the holder, and the measurement, the total error in the determination of the magnetization of the sample does not exceed 5%.

The temperature dependences of the magnetization of the sample in a weak residual field of the magnet and in a strong magnetic field of 5 T are shown in Fig. 5. The temperature dependence of the magnetization measured in a weak residual field of 0.025 T clearly demonstrates a magnetic transition with the critical temperature $T = 37$ K. The magnetic transition temperature is determined at the point where the slope of the curve $M(T)$ reaches the maximum value. This temperature is 6 K below the corresponding critical temperature of the initial compound $Co_3O_2BO_3$. In a magnetic field of 5 T, the magnetic transition is strongly smeared over the temperature range.

The temperature dependence of the inverse magnetic susceptibility in the paramagnetic region obeys the Curie–Weiss law: $\chi = C/(T - \Theta)$. The approximation of the experimental data according to the Curie–Weiss law is presented in the inset to Fig. 5. The paramagnetic constant $C = 0.019$ cm^3 K/g corresponds to the effective magnetic moment $\mu_{eff} = 6.44\mu_B$ per formula unit or $3.72\mu_B$ per metal ion. Taking into account that 20% of the metal ions (Ga^{3+}) are nonmagnetic, we find the magnetic moment $4.18\mu_B$ for each magnetic cobalt ion. This value almost completely coincides with the corresponding effective magnetic moment obtained in our previous work [14] for the unsubstituted cobalt ludwigite $Co_3O_2BO_3$. The paramagnetic Curie temperature is $\Theta = 14$ K.

The magnetization curves measured in strong magnetic fields of up to 14 T differ significantly from each other in different directions of the magnetic field with respect to the crystallographic axes. In the crystallographic *c* direction, the magnetization is relatively small and the dependence $M(H)$ is almost linear for all the studied temperatures (Fig. 6). According to these data, the crystallographic *c* direction (along the crystal needle) coincides with the hard magnetization axis. The magnetic moment of the sample lies in the *ab* plane.

The magnetization curves of the sample in the magnetic field oriented along the crystallographic directions *a* and *b* in the cross section of the crystal are similar to each other for both the high and low temperatures (Fig. 7). Let us consider in more detail the magnetization curves along the crystallographic *a* direction (Fig. 8). The magnetization isotherms below the magnetic ordering temperature are presented in Fig. 8a. Figure 8b shows a family of magnetization curves above the critical temperature. The latter dependences are typical of the paramagnetic state of the sample. At temperatures below the magnetic transition point, the magnetization curves are irreversible and do not reach saturation. In the high-field range, all the magnetization curves obtained at temperatures $T \le 20$ K are linear and almost completely coincide with each other. The extrapolation of the magnetization curve by a linear dependence is shown in the iso-

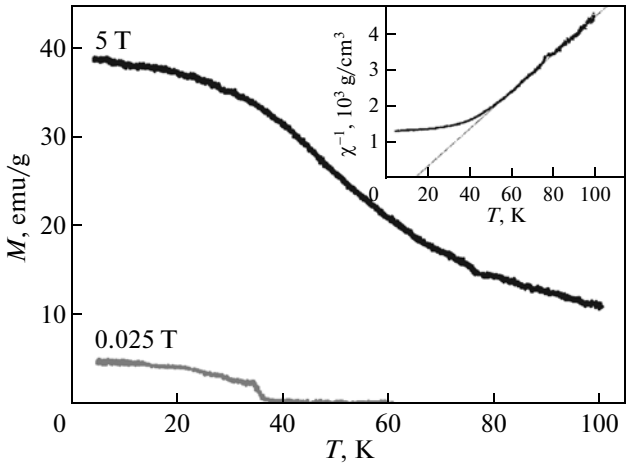

Fig. 5. Temperature dependences of the magnetization of the $Co_{2.4}Ga_{0.6}O_2BO_3$ crystal measured in the ZFC mode. The heating is performed in two magnetic fields. The magnetic field is directed along the crystallographic *a* axis. The inset shows the temperature dependence of the inverse magnetic susceptibility corresponding to the curve $M(H)$ measured in a magnetic field $H = 5$ T. The straight line is the approximation according to the Curie–Weiss law.

therm $M(H)$ for $T = 1.8$ K (Fig. 8a). The magnetic susceptibility corresponding to the contribution linear in the magnetic field is $\chi_{AF} = 1.3 \times 10^{-4}$ cm^3/g.

If the magnetic moments of all the cobalt ions were to be oriented along the magnetic field, then, for each ion in the unsubstituted cobalt ludwigite $Co_3O_2BO_3$ at saturation, there should be, on the average, the magnetic moment $\mu = g\langle J\rangle\mu_B$. Here, the question arises as to the magnitude of the total angular momentum J and the value of the g-factor for cobalt ions in the divalent and trivalent states. The Co^{3+} and Co^{2+} ions in a cubic crystal field have a nonzero orbital angular momentum $\tilde{l} = 1$. Taking into account the spin–orbit coupling, we can determine the total angular momenta and the effective g-factors [21]. For the Co^{3+} ion, we obtain $S = 2$, $\tilde{l} = 1$, $\tilde{J} = 1$, and $g_J = 3.5$. For the Co^{2+} ion, we have $S = 3/2$, $\tilde{l} = 1$, $\tilde{J} = 1/2$, and $g_J = 4.33$. As a result, the average magnetic moment per cation in the unsubstituted crystal of the cobalt ludwigite $Co_3O_2BO_3$ with the ratio $Co^{2+} : Co^{3+} = 2 : 1$ in the saturation state should be equal to

$$\mu = \frac{1}{3}(2\mu_{Co^{2+}} + \mu_{Co^{3+}})$$

$$= \frac{1}{3}\left(2 \times 4.33 \times \frac{1}{2} + 1 \times 3.5\right)\mu_B = 2.61\mu_B.$$

For the substituted composition $Co_{2.4}Ga_{0.6}O_2BO_3$, we can approximately assume that the nonmagnetic gallium ions substitute for one-half of the trivalent cobalt ions. Then, we have $Co^{2+} : Co^{3+} = 4 : 1$ and

$$\mu = \frac{1}{5}(4\mu_{Co^{2+}} + \mu_{Co^{3+}})$$

$$= \frac{1}{5}\left(4 \times 4.33 \times \frac{1}{2} + 1 \times 3.5\right)\mu_B = 2.43\mu_B.$$

The spontaneous magnetic moment determined from the magnetization curves presented in Fig. 8 for the $Co_{2.4}Ga_{0.6}O_2BO_3$ compound is equal to $0.58\mu_B$ per metal ion or $0.73\mu_B$ per cobalt ion, which is considerably smaller than the maximum possible value equal to $2.43\mu_B$. The remanent magnetization can be determined from the reversal of the curve $M(H)$. At a temperature $T = 1.8$ K, the remanent magnetization is found to be $0.59\mu_B$ per cobalt ion, which accounts for 81% of the spontaneous magnetic moment or 24% of the maximum possible value.

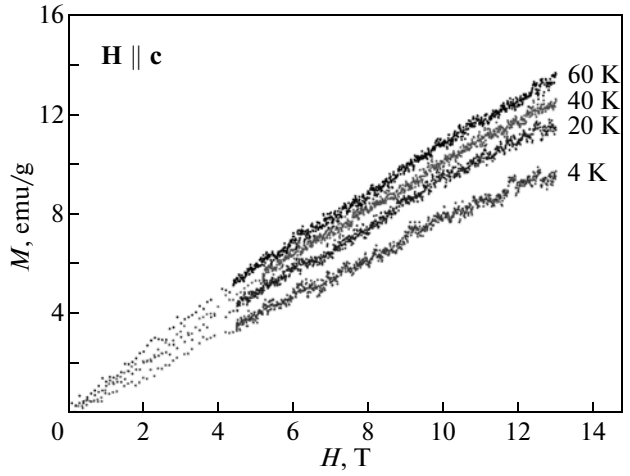

Fig. 6. Magnetization isotherms measured above and below the magnetic ordering temperature in the crystallographic *c* direction (along the needle).

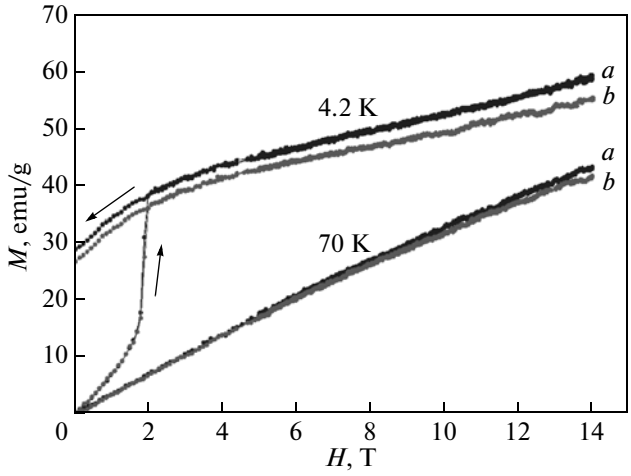

Fig. 7. Comparison of the magnetization isotherms in the crystallographic directions *a* and *b* above ($T = 70$ K) and below ($T = 4.2$ K) the magnetic transition temperature.

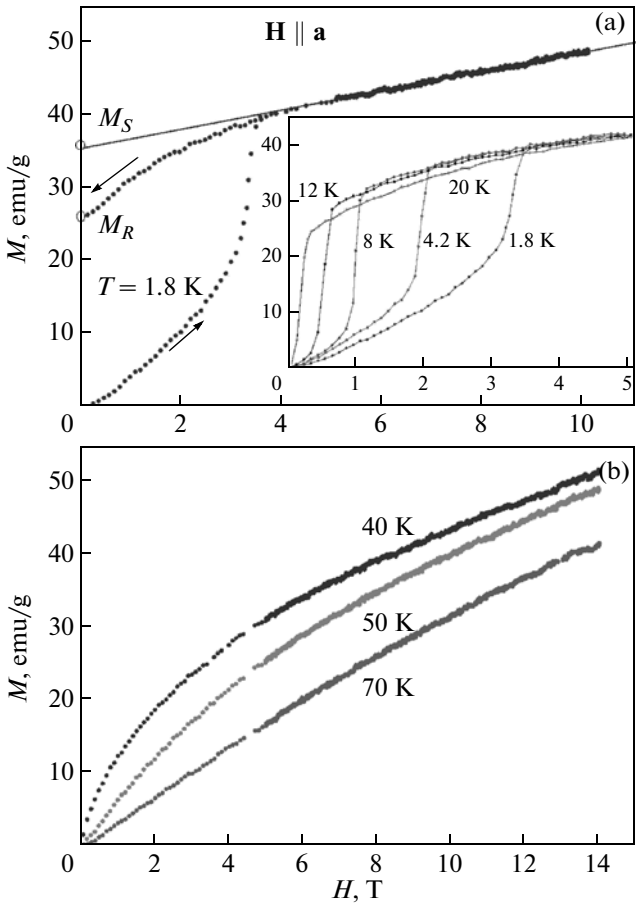

Fig. 8. Magnetization curves measured in the crystallographic *a* direction at different temperatures: (a) the magnetically ordered phase and (b) the paramagnetic phase. The inset shows the magnetization curves plotted in the same coordinates as the curves in the main figure. Designations: M_S is the spontaneous magnetization, and M_R is the remanent magnetization.

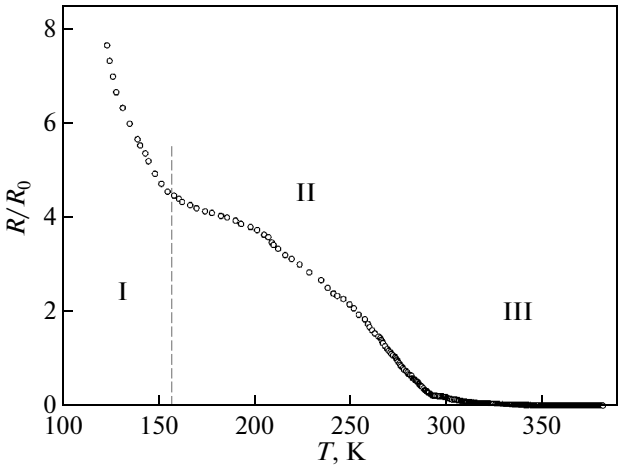

Fig. 9. Temperature dependence of the electrical resistance normalized to the value of R_0 at 0°C for the $Co_{2.4}Ga_{0.6}O_2BO_3$ sample. Portions I–III of the curve correspond to different modes of the behavior of the electrical resistance.

5. ELECTRICAL RESISTANCE

The vast majority of transition metal oxyborates at low temperatures belong to the class of magnetic dielectrics [22]. With an increase in the temperature, the electrical conduction is usually activated. The electron transport rather frequently occurs according to the Mott's variable-range hopping mechanism [23]. The electrical resistance in this case depends on the temperature as $R = R'\exp(\Delta/kT^{1/4})$ [24], where R' and Δ are the Mott's parameters determined by the density of states and the other parameters of the electronic structure. The electrical resistance of the samples often remains relatively large in the absolute value (more than 1 MΩ) to room temperature. These data, in combination with small sizes of the samples, make it difficult to perform correct measurements of the electrical resistance with the use of the four-point probe method. Therefore, one has to use a simpler two-point probe technique and to put up with the possible presence of the contribution from the near-contact regions to the measured value of the electrical resistance. Such a technique for measuring the electrical resistance was used in our case. The electrical resistance was measured along the long axis of the crystal with the use of an automated complex intended for transport and magnetotransport measurements and an E6-13A teraohmmeter.

The electrical resistance of the sample at room temperature was found to be 8 GΩ, which corresponds in the order of magnitude to the electrical resistivity of 10 Ω cm. This value is typical of oxyborates [2, 22, 23]. The temperature dependence of the electrical resistance normalized to the value of R_0 at 0°C for the $Co_{2.4}Ga_{0.6}O_2BO_3$ sample is shown in Fig. 9. In accordance with the behavior of the temperature dependence of the electrical resistance, the temperature range from 120 to 400 K, in which the electrical resistance was measured, can be divided into three portions. Portion I corresponds to the low-temperature measurements of the electrical resistance in the range from 120 to 160 K. In this range, the electrical resistance rapidly increases with a decrease in the temperature, and the sample undergoes dielectrization. In our case, the electrical resistance measurements were performed down to $T_{min} = 120$ K. Below this temperature, the electrical resistance of the sample is so great that attempts to measure it have no sense. This behavior of the electrical resistance at low temperatures, in general, is characteristic of the class of oxyborate compounds [2, 21, 22].

Portion III corresponds to the high-temperature measurements of the electrical resistance in the range from 290 to 400 K. Portion II (in the range from 160 to 290 K) is the transition region. Figure 10 shows the dependence of the logarithm of the normalized electrical resistance of the $Co_{2.4}Ga_{0.6}O_2BO_3$ sample on the

inverse temperature. The designations of the regions corresponding to different modes of the behavior of the electrical resistance are the same as in Fig. 9. In portions I and III, the electrical resistance exhibits an almost linear behavior. In portion II, the temperature dependence of the electrical resistance has a sharply nonlinear behavior. This indicates that there exists a transition in the mechanism of charge transport. The transition temperature T_c can be determined in accordance with the maximum change in the derivative of the function $\ln(R/R_0)$ with respect to the temperature. The corresponding dependence is shown in the inset to Fig. 10. It can be seen that the transition temperature is $T_c \approx 280$ K.

The almost linear behavior of the electrical resistance as a function of the inverse temperature (Fig. 10) justifies the attempt to consider it in terms of the activation conduction. The high-temperature and low-temperature branches of the electrical resistance were approximated by the simple Arrhenius activation law. The obtained activation energies of electrical conduction are found to be as follows: 1.25 eV in the high-temperature range and 0.04 eV in the low-temperature range.

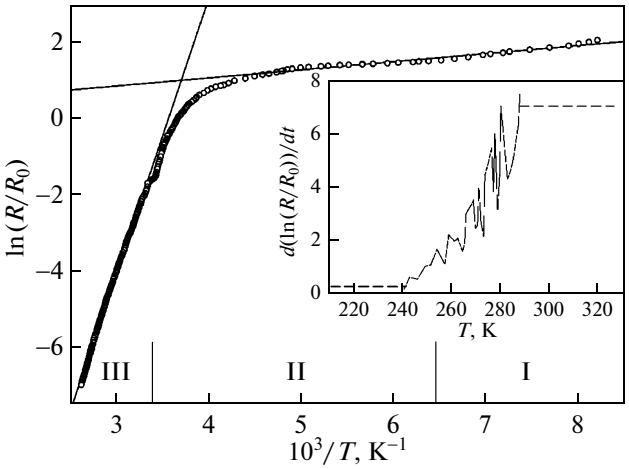

Fig. 10. Dependence of the logarithm of the normalized electrical resistance of the $Co_{2.4}Ga_{0.6}O_2BO_3$ sample on the inverse temperature. Roman numerals indicate regions corresponding to different modes of the behavior of the electrical resistance. Straight lines represent the approximation according to the activation law. The inset shows the derivative of the logarithm of the electrical resistance with respect to the temperature in the region of changes in the electrical conduction mechanisms.

6. DISCUSSION OF THE RESULTS

The processes performed in our present work for the synthesis of the substituted cobalt ludwigites based on the $Co_3O_2BO_3$ compound demonstrated that gallium is readily soluble in the mixture $Bi_2Mo_3O_{12} : B_2 : CoO : Na_2Co_3 : Co_2O_3$, which can be responsible for the high degree of substitution of the transition metal ion.

The exact distribution of the metal ions over the crystallographic positions in accordance with their valence state in the cobalt ludwigite is currently unknown. In the isostructural analogue $Fe_3O_2BO_3 : Ga$, sites *1* and *3* are occupied by the divalent ions, while the nominally trivalent ions located in sites *2* and *4* share among themselves a single "excess" electron. The degree of localization of this electron, according to the neutron diffraction data, strongly depends on the temperature [5]. For the cobalt ludwigite, the valences of cobalt ions in different sites were determined using the bond-valence-sum method [13, 19]. Based on this method, it can be assumed that the valences of cobalt ions in sites *1–3* and *4* are equal to 2+ and 3+, respectively.

According to the X-ray diffraction data, the trivalent gallium ion, with a special preference, is located in one of the nonequivalent crystallographic positions (site *4*). In this site, the trivalent gallium ion substitutes for the trivalent cobalt ion Co^{3+}. It is interesting to note that it is this site which, every time, appears to be most preferred for different substituting ions. We observed this tendency previously in the cases where cobalt is substituted for by iron [6, 17], copper [18], and manganese [19]. It is known that, in these cases, iron also resides in the trivalent state, while manganese exhibits a variable valence (2+ and 3+). The valence state of copper remains unknown; however, the copper ion in these compounds exhibits a valence of 2+ rather more frequently than a valence of 3+. Site *4* stands out among the other sites by the following features: (1) it is located in the center of the zig-zag wall; (2) it has the smallest isotropic thermal parameter; and (3) it is characterized by the smallest electric field gradient across the oxygen octahedron. In other words, the metal ion located in this site has the most symmetric environment. This site should be the most favorable for the ions with a symmetric electron shell, for example, for the d^5 and d^{10} ions. These ions are the Fe^{3+} and Ga^{3+} ions, respectively. It is these ions which exhibit the most pronounced preference for site *4*. In the case where cobalt is substituted for by manganese, which is involved in both the divalent (d^5) and trivalent (d^4) states, the preference for this site is pronounced considerably weaker.

Apart from sites *4*, the Ga^{3+} ions in small amounts occupy sites *2*, thus forming layers aligned parallel to the crystallographic *ab* plane. These layers are separated by the other layers containing only the magnetic cobalt ions.

The introduction of gallium into the cobalt ludwigite leads to a small increase in the unit cell parameters and interionic distances. This can be caused by two factors. First, the ionic radius of Ga^{3+} (0.62 Å) is slightly larger than the ionic radius of Co^{3+} (0.61 Å). Second, if a part of the trivalent gallium ions displaces the Co^{2+} ions from sites *2*, then, under the conditions of charge balance, these ions with a larger ionic radius (0.745 Å) should occupy sites *4*, which is not

characteristic of them. This can lead to an increase in the degree of distortion in the lattice, which is accompanied by a slight increase in the lattice volume.

As regards the effect of the diamagnetic dilution on the magnetic properties of the cobalt ludwigite, in this work, we obtained the two main results. The first of them is quite predictable: the introduction of gallium into the original material leads to a weakening of the magnetic interactions, as well as to a decrease in the temperature of the magnetic transition. In this case, the character of the magnetic order at a given gallium concentration presumably remains the same as in the original compound $Co_3O_2BO_3$. Judging from the temperature and magnetic-field dependences of the magnetization, the $Co_{2.4}Ga_{0.6}O_2BO_3$ compound is a ferrimagnet with the magnetic moment oriented in the crystallographic *ab* plane. The values of the magnetic moment significantly differ from those corresponding to saturation, thus indicating its substantial compensation.

The second result, which was obtained from the magnetic measurements, is somewhat unexpected: the magnetic anisotropy in the *ab* plane almost completely disappears. In the original material, the magnetic anisotropy in this plane is extremely pronounced. The $Co_3O_2BO_3$ compound is an easy-axis ferrimagnet in which the easy magnetization axis coincides with the crystallographic *b* direction. The $Co_{2.4}Ga_{0.6}O_2BO_3$ compound studied in the present work can be attributed to ferrimagnets of the "easy plane" type. There are grounds to assume that the magnetic anisotropy in the cobalt ludwigite $Co_3O_2BO_3$ is determined predominantly by the transition metal ions located in nonequivalent crystallographic sites *4*, because it is these ions which were subjected to the nonmagnetic substitution. According to the results obtained in our work, the magnetic anisotropy in the cobalt ludwigite, most likely, has an exchange nature.

In the paramagnetic state, the effect of gallium ions on the effective magnetic moment is reduced to a simple diamagnetic dilution. The decrease in the magnetic moment is in exact agreement with the amount of introduced nonmagnetic ions. As regards the paramagnetic Curie–Weiss temperature Θ, in the initial composition $Co_3O_2BO_3$, as well as in any anisotropic magnetic material, this temperature strongly depends on the direction of the magnetic field with respect to the anisotropy axes. When the measurements were performed in the *a* direction, we obtained the paramagnetic Curie–Weiss temperature $\Theta \approx -20$ K [6] for the unsubstituted composition and $\Theta = 16$ K for the gallium-substituted composition. These values are not very different from zero but have the opposite sign. This indicates a change in the predominant exchange interactions upon the substitution. Nonetheless, it can be concluded that the substitution of gallium for 20% of the cobalt ions does not substantially affect their behavior in the paramagnetic phase.

In the temperature dependence of the electrical resistance of the $Co_{2.4}Ga_{0.6}O_2BO_3$ compound, there is a broad transition region observed at temperatures in the range from 160 to 290 K. On both sides of the transition region, the dependence of the logarithm of the electrical resistance on the inverse temperature has an almost linear behavior, which can indicate the occurrence of activation conduction. However, the low-temperature branch of the dependence $R(T)$ demonstrates a considerably more rapid increase in the electrical resistance with a decrease in the temperature as compared to the high-temperature branch. The approximation performed in accordance with a simple exponential law gives a low value of the activation energy $E_{a1} = 0.04$ eV in the low-temperature range and a substantially higher value of the activation energy $E_{a2} = 1.25$ eV in the high-temperature range. These values suggest that, in this composition, the impurity mechanism of electrical conduction coexists with the intrinsic mechanism. The band gap is $\Delta E = 2E_{a2} = 2.5$ eV. Moreover, near the edges of the band gap, there are impurity levels or a narrow band at a depth of 0.04 eV. This experimental result is in contradiction with the extended Hückel tight binding (EHTB) calculations performed for the electronic structure of the $Co_3O_2BO_3$ compound in [25]. According to these calculations, the band structure of the $Co_3O_2BO_3$ compound has no semiconductor gap, and this compound should exhibit metallic conductivity. The electrical conductivity observed in our present work is far from metallic both in the base compound $Co_3O_2BO_3$ [2] and in the substituted composition $Co_3O_2BO_3$: Ga. At the same time, we did not reveal a strong correlation between changes in the magnetic order and the electronic structure [26, 27], which is characteristic of magnetic semiconductors.

7. CONCLUSIONS

The performed investigations of the structural, magnetic, and transport properties of the substituted cobalt ludwigite $Co_{2.4}Ga_{0.6}O_2BO_3$ have revealed that the substituted composition is isostructural with the original material of the $Co_3O_2BO_3$ composition, but with slightly greater interionic distances. The Ga^{3+} ions exhibit a strong preference in the occupation of one of the four nonequivalent crystallographic positions in the ludwigite structure. It is the position characterized by the smallest values of the isotropic displacement parameter and the electric field gradient of the oxygen octahedron. This situation is similar to the case where trivalent iron ions Fe^{3+} are introduced into the cobalt ludwigite. Both of the substituting ions have a symmetric electronic structure (d^{10} in Ga^{3+} and d^5 in Fe^{3+}).

In the paramagnetic region, the substitution of gallium ions for cobalt ions brings about the effect of conventional diamagnetic dilution, which leads to a decrease in the effective magnetic moment. The mag-

netic ordering is achieved at a temperature of 37 K, i.e., by 6 K lower than the magnetic ordering temperature of the original material. The hypothetically ferrimagnetic type of magnetic ordering upon the substitution remains unchanged; however, the uniaxial magnetic anisotropy, which is clearly pronounced in the cobalt ludwigite $Co_3O_2BO_3$, disappears. The substituted material has a magnetic anisotropy of the easy plane type (this easy plane coincides with the crystallographic *ab* plane).

The electrical resistance of the $Co_{2.4}Ga_{0.6}O_2BO_3$ compound demonstrates an activation character of the behavior in both the low-temperature and high-temperature ranges. However, the activation energy for electrical conduction does not remain constant. In the transition range from 160 to 290 K, this activation energy changes by a factor of approximately 30. Such a situation can take place upon the transition from impurity conduction to intrinsic conduction with an increase in the temperature. The formation of the impurity band, most likely, occurs as a result of the introduction of gallium ions into the original material. The contribution from Mott's variable-range hopping conduction is also not ruled out.

ACKNOWLEDGMENTS

This study was supported by the Council on Grants from the President of the Russian Federation for Support of Leading Scientific Schools of the Russian Federation (grant no. NSh-1044.2012.2) and the Russian Foundation for Basic Research (project nos. 12-02-00175-a and 12-02-00470-a).

REFERENCES

1. N. B. Ivanova, A. D. Vasil'ev, D. A. Velikanov, N. V. Kazak, S. G. Ovchinnikov, G. A. Petrakovskii, and V. V. Rudenko, Phys. Solid State **49** (4), 651 (2007).
2. N. V. Kazak, N. B. Ivanova, V. V. Rudenko, S. G. Ovchinnikov, A. D. Vasilyev, and Yu. V. Knyazev, Solid State Phenom. **152–153**, 104 (2009).
3. G. A. Petrakovskii, L. N. Bezmaternykh, D. A. Velikanov, A. M. Vorotynov, O. A. Bayukov and M. Schneider, Phys. Solid State **51** (10), 2077 (2009).
4. D. C. Freitas, M. A. Continentino, R. B. Guimaraes, J. C. Fernandes, E. P. Oliveira, R. E. Santelli, J. Ellena, G. G. Eslava, and L. Ghivelder, Phys. Rev. B: Condens. Matter **79**, 134437 (2009).
5. F. Bordet and E. Suard, Phys. Rev. B: Condens. Matter **79**, 144408 (2009).
6. N. B. Ivanova, N. V. Kazak, Yu. V. Knyazev, D. A. Velikanov, L. N. Bezmaternykh, S. G. Ovchinnikov, A. D. Vasiliev, M. S. Platunov, J. Bartolomé, and G. S. Patrin, JETP **113** (6), 1015 (2011).
7. F. S. Sarrat, R. B. Guimaraes, M. A. Continentino, J. C. Fernandes, A. C. Doriguetto, and J. Ellena, Phys. Rev. B: Condens. Matter **71**, 224413 (2005).
8. M. S. Platunov, N. B. Ivanova, N. V. Kazak, and S. G. Ovchinnikov, J. Sib. Fed. Univ. **4** (4), 298 (2011).
9. S. R. Bland, M. Angst, S. Adiga, V. Scagnoli, R. D. Johnson, J. Herrero-Martin, and P. D. Hatton, Phys. Rev. B: Condens. Matter **82**, 115110 (2010).
10. J. A. Hriljac, R. D. Brown, A. K. Cheetham, and L. C. Satek, J. Solid State Chem. **84**, 289 (1990).
11. M. A. Continentino, J. C. Fernandes, R. B. Guimaraes, H. A. Borges, A. Sulpice, J.-L. Tholence, J. L. Siquera, J. B. M. da Gunha, and C. A. dos Santos, Eur. Phys. J. B **9**, 613 (1999).
12. H. Neuendorf and W. Gunber, J. Magn. Magn. Mater. **173**, 117 (1997).
13. D. C. Freitas, M. A. Continentino, R. B. Guimaraes, J. C. Fernandes, J. Ellena, and L. Ghivelder, Phys. Rev. B: Condens. Matter **77**, 184422 (2008).
14. J. Bartolome, A. Arauzo, N. V. Kazak, N. B. Ivanova, S. G. Ovchinnikov, Yu. V. Knyazev, and I. S. Lyubutin, Phys. Rev. B: Condens. Matter **83**, 144426 (2011).
15. D. C. Freitas, R. B. Guimaraes, D. R. Sanchez, J. C. Fernandes, M. A. Continentino, J. Ellena, A. Kitada, H. Kageyama, A. Matsuo, K. Kindo, G. G. Eslava, and L. Ghivelder, Phys. Rev. B: Condens. Matter **81**, 024432 (2010).
16. N. B. Ivanova, M. S. Platunov, Yu. V. Knyazev, N. V. Kazak, L. N. Bezmaternykh, E. V. Eremin, and A. D. Vasiliev, Low Temp. Phys. **38** (2), 172 (2012).
17. N. V. Kazak, N. B. Ivanova, O. A. Bayukov, S. G. Ovchinnikov, A. D. Vasiliev, V. V. Rudenko, J. Bartolome, A. Arauzo, and Yu. V. Knyazev, J. Magn. Magn. Mater. **323**, 521 (2011).
18. N. B. Ivanova, N. V. Kazak, Yu. V. Knyazev, D. A. Velikanov, A. D. Vasiliev, L. N. Bezmaternykh, M. S. Platunov, and S. G. Ovchinnikov, Physica B (Amsterdam) (2012) (in press).
19. Yu. V. Knyazev, N. B. Ivanova, N. V. Kazak, M. S. Platunov, L. N. Bezmaternykh, D. A. Velikanov, A. D. Vasiliev, S. G. Ovchinnikov, and G. Yu. Yurkin, J. Magn. Magn. Mater. **324**, 923 (2012).
20. V. I. Nizhankovskii and L. B. Lugansky, Meas. Sci. Technol. **18** (5), 1533 (2007).
21. A. Abragam and B. Bleaney, *Electron Paramagnetic Resonance of Transition Ions* (Oxford University Press, Oxford, 1970; Mir, Moscow, 1972).
22. N. V. Kazak, S. G. Ovchinnikov, M. Abd-Elmegiud, and N. B. Ivanova, Physica B (Amsterdam) **359–361**, 1324 (2005).
23. A. D. Balaev, O. A. Bayukov, A. D. Vasil'ev, D. A. Velikanov, N. B. Ivanova, N. V. Kazak, S. G. Ovchinnikov, M. Abd-Elmegiud, and V. V. Rudenko, JETP **97** (5), 989 (2003).
24. N. F. Mott, *Metal–Insulator Transitions* (Taylor and Francis, London, 1974; Nauka, Moscow, 1979).
25. M. Matos, arXiv:1009.5899v1 cond-mat.mtrl-sci. (2010).
26. E. L. Nagaev, *Physics of Magnetic Semiconductors* (Nauka, Moscow, 1979; Mir, Moscow, 1983).
27. S. G. Ovchinnikov, Phase Transform. **36**, 15 (1991).

Translated by O. Borovik-Romanova